

Supporting Information for

**Direct fabrication of bi-metallic PdRu nanorod assemblies
for electrochemical ammonia synthesis**

Hongjing Wang, Yinghao Li, Dandan Yang, Xiaoqian Qian, Ziqiang Wang, You Xu, Xiaonian Li,

Hairong Xue*, Liang Wang*

State Key Laboratory Breeding Base of Green-Chemical Synthesis Technology, College of
Chemical Engineering, Zhejiang University of Technology, Hangzhou, Zhejiang 310014, P. R.
China.

*Corresponding authors: xuehairong@zjut.edu.cn; wangliang@zjut.edu.cn

Experimental Section

Calibration reference electrode:

An Ag/AgCl electrode is used as the reference electrode in all measurements and the reference electrode was calibrated on reversible hydrogen electrode (RHE). The calibration process was performed based on form literature (S1), all the potentials were calibrated according to the formula of $E(\text{RHE}) = E(\text{Ag/AgCl/saturated KCl}) + 0.28 \text{ V}$ in this study.

Calculation of double-layer capacitance:

The electrochemically effective surface areas are reflected by double layer capacitances (C_{dl}), which can be calculated from cyclic voltammograms (CVs). CVs were performed at which no obvious Faradic current were observed. The capacitive currents, $\Delta j/2$ ($\Delta j = j_a - j_c$, j_a and j_c refer to anodic and cathodic current values at 0.42 V vs. RHE, were plotted against the scan rate. The linear relationships were observed with the slopes of the C_{dl} value.

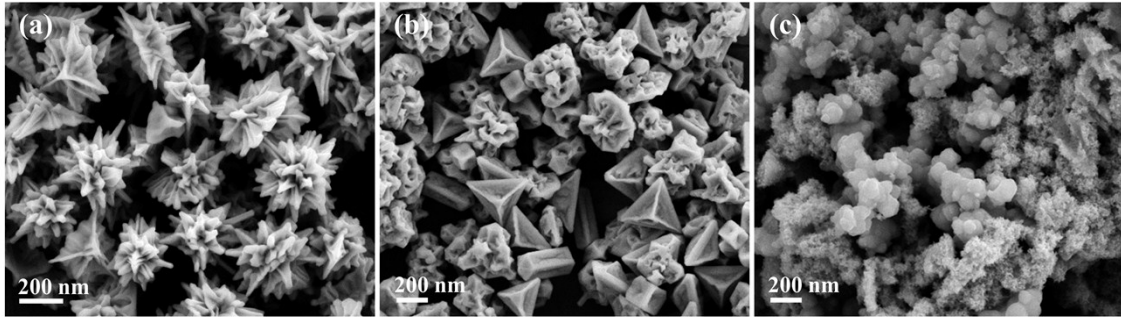


Fig. S1 SEM images of the samples prepared under the identical conditions used for the typical synthesis in the absence of KBr (a), and by replacing KBr with KCl (b) and KI (c), respectively.

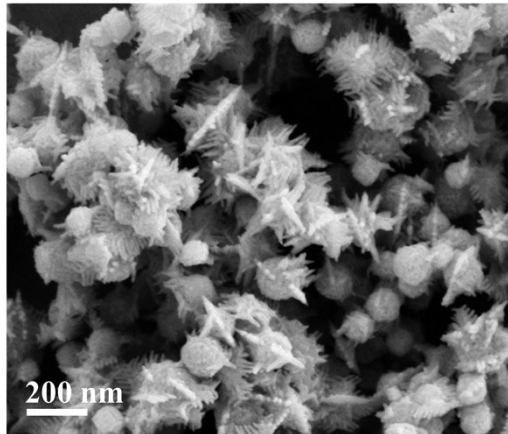


Fig. S2 SEM image of the sample prepared without HCl.

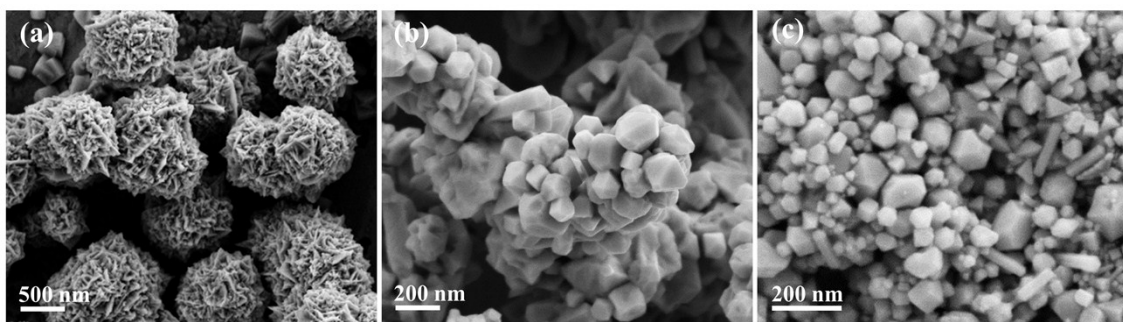


Fig. S3 SEM images of the samples prepared under the typical conditions without F127 (a), and by replacing F127 with DM-970 (b), and Brij 58 (c), respectively.

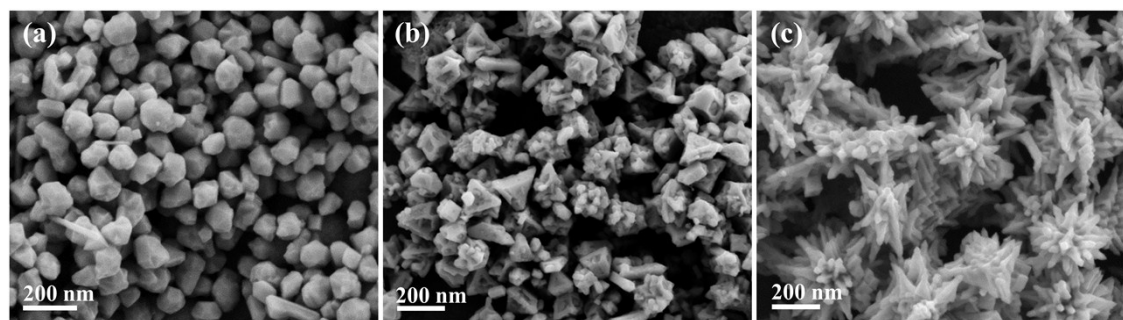


Fig. S4 (a) SEM image of the Pd NPs prepared without Ru precursor. (b and c) SEM images of the PdRu NPs and PdRu NDs prepared with the different metallic precursor amounts under identical conditions used for the typical synthesis. The added metallic precursor amounts of Na_2PdCl_4 and RuCl_3 are 3.9 mL and 0.6 mL for PdRu NPs and 1.1 mL and 3.4 mL for PdRu NDs, respectively.

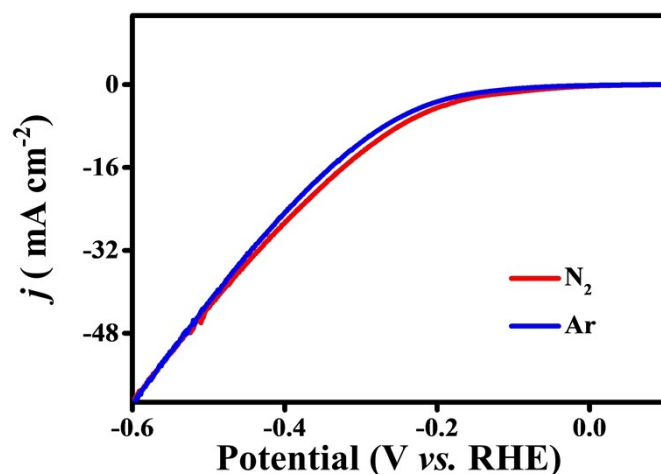


Fig. S5 LSV curves of the PdRu NRAs in a N_2 -saturated (red line) and an Ar-saturated (blue line) 0.1 M HCl electrolyte at 50 mV s^{-1} .

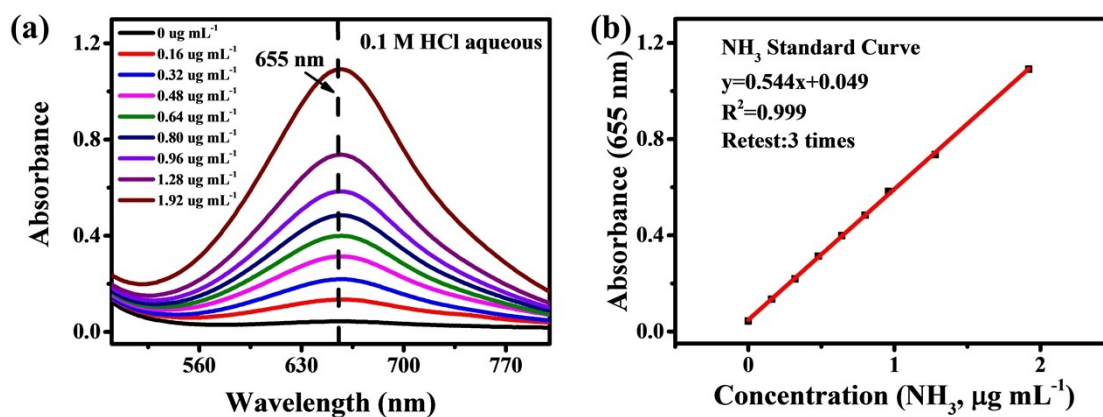


Fig. S6 Absolute calibration of the indophenol blue method using ammonium chloride solutions of known concentration as standards. (a) UV-Vis curves of indophenol assays with NH_4^+ ions after incubated for 2 h at room temperature, (b) calibration curve used for estimation of NH_3 by NH_4^+ ion concentration. The absorbance at 655 nm was measured by UV-Vis spectrophotometer, and the fitting curve shows good linear relation of absorbance with NH_3 concentration ($y = 0.544x + 0.049$, $R^2 = 0.999$) of three times independent calibration curves.

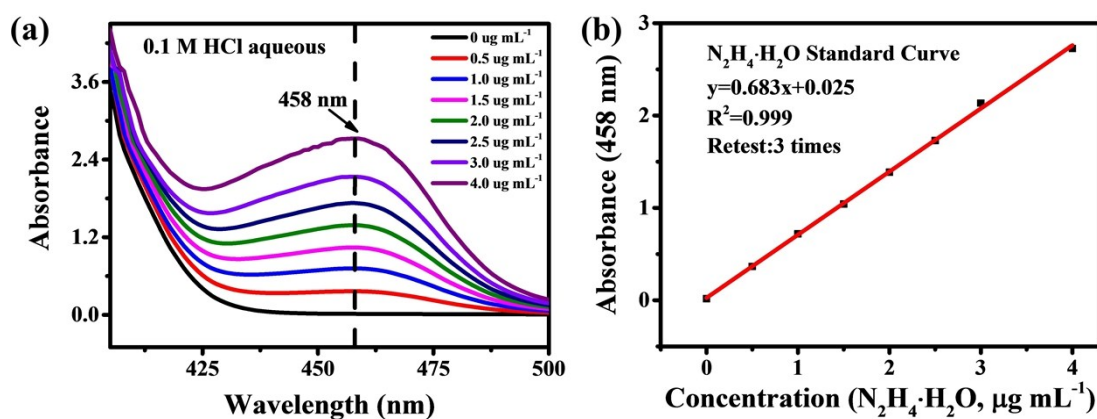


Fig. S7 Absolute calibration of the Watt and Chrisp (para-dimethylaminobenzaldehyde) method for the estimating of $\text{N}_2\text{H}_4\cdot\text{H}_2\text{O}$ concentration using $\text{N}_2\text{H}_4\cdot\text{H}_2\text{O}$ solutions with known concentration as standards. (a) UV-Vis curves of various $\text{N}_2\text{H}_4\cdot\text{H}_2\text{O}$ concentration after incubated for 10 min at room temperature, (b) calibration curve used for estimation of $\text{N}_2\text{H}_4\cdot\text{H}_2\text{O}$ concentration. The absorbance at 458 nm was measured by UV-Vis spectrophotometer, and the fitting curve shows good linear relation of absorbance with $\text{N}_2\text{H}_4\cdot\text{H}_2\text{O}$ concentration ($y = 0.683x + 0.025$, $R^2 = 0.999$) of three times independent calibration curves.

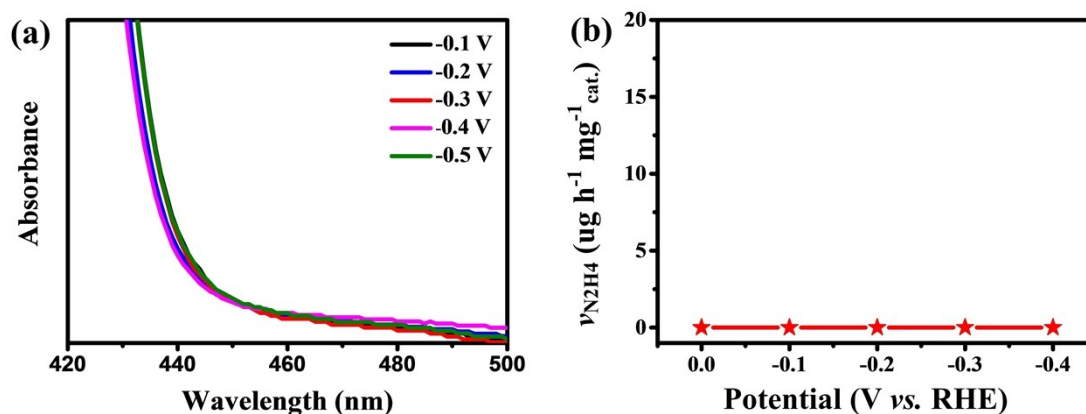


Fig. S8 (a) UV-vis absorption spectra of the HCl electrolyte stained with the Watt and Chrisp (para-dimethylaminobenzaldehyde) indicator after charging at each given potential for 2 h. (b) Yield rate of $\text{N}_2\text{H}_4\cdot\text{H}_2\text{O}$ formation at each given potential.

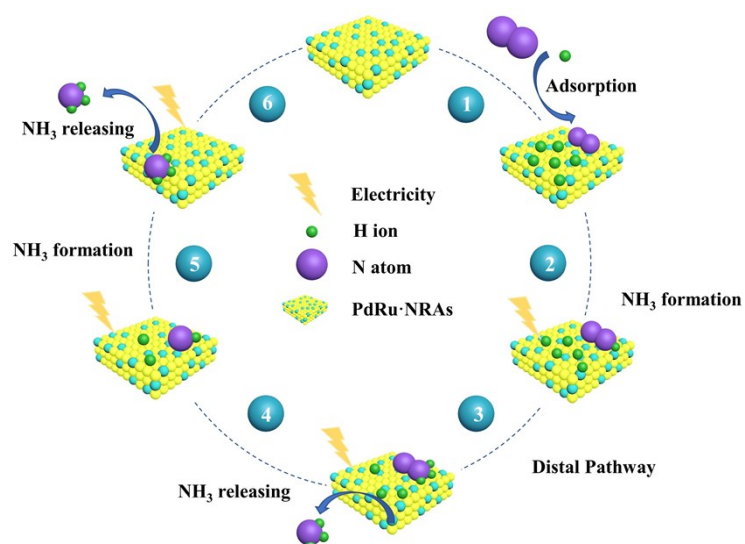


Fig. S9 The proposed pathway for the NH_3 synthesis using PdRu NRAs catalyst.

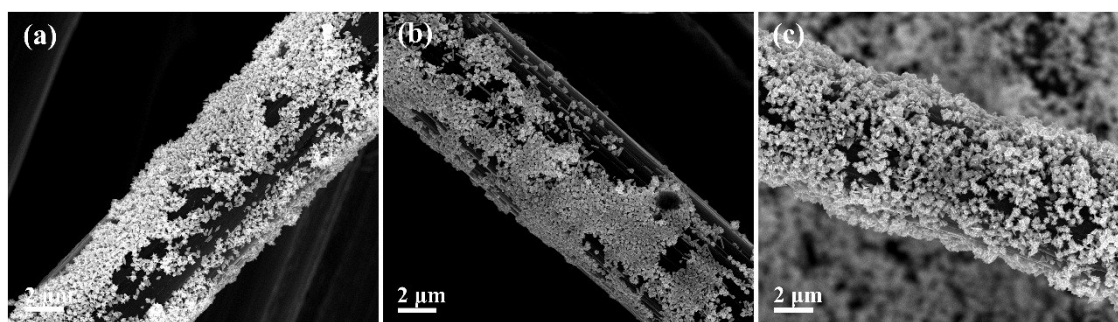


Fig. S10 SEM images of the different samples loaded onto a carbon paper electrode with area of $0.5 \times 0.5 \text{ cm}^2$: (a) PdRu NRAs, (b) PdRu NPs, (c) PdRu NDs.

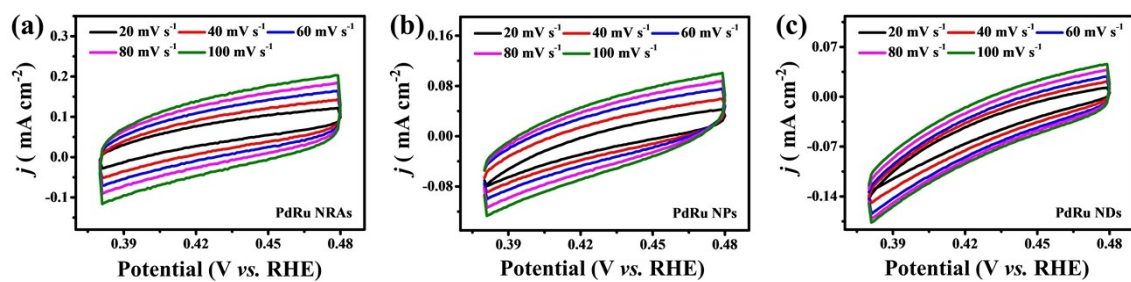


Fig. S11 (a-c) Cyclic voltammograms for synthesized PdRu NRAs, PdRu NDs and PdRu NPs in 0.1 M HCl solution with a potential range of 0.38V~0.48V vs. RHE.

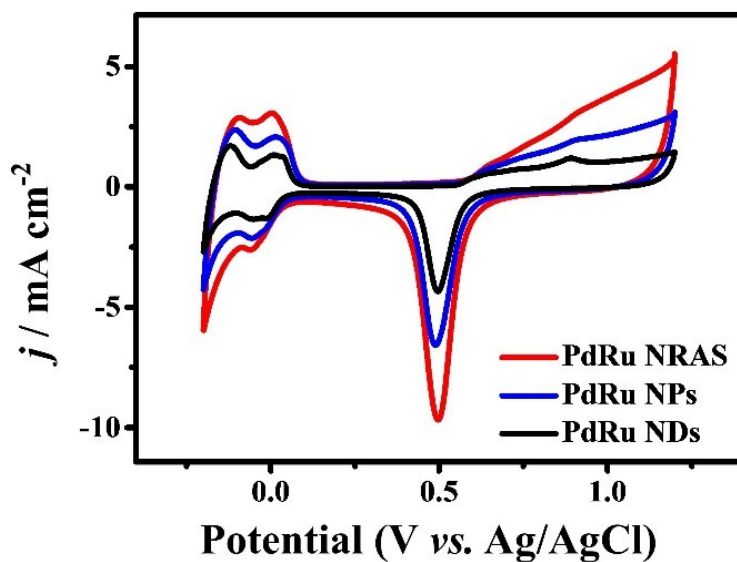


Fig. S12 CV curves of the catalysts in 0.5 M H₂SO₄ solution under a sweep rate of 50 mV s⁻¹ (potential range: -0.2V~1.2V vs. Ag/AgCl).

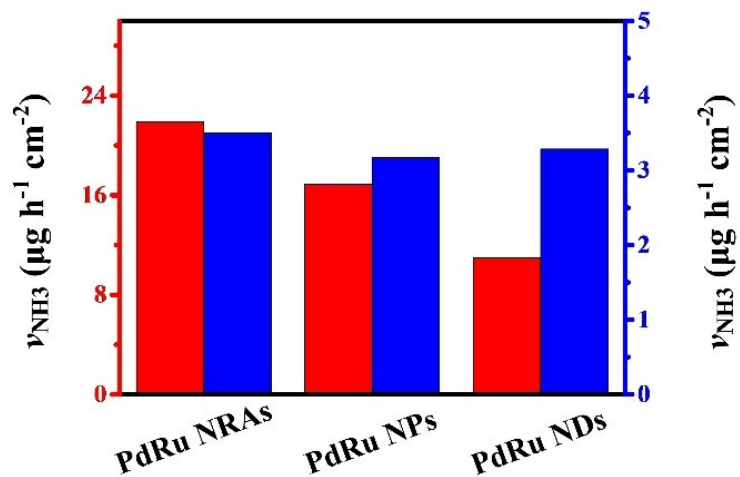


Fig. S13 Yield rate of NH₃ calculated by ECSA (blue) and electrode area (red) of the samples.

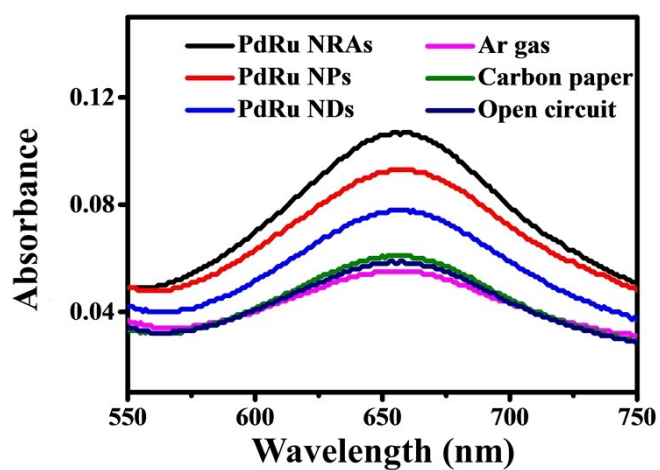


Fig. S14 UV-vis absorption spectra of the HCl electrolyte stained with indophenol indicator after charging at -0.2 V for 2 h under various conditions.

Table S1. The comparisons of the NRR performance of the PdRu NRAs with the recently reported catalysts under ambient conditions.

Catalyst	Electrolyte	Conditions	Yield.	Ref.
PdRu NRAs	0.1 M HCl	25 °C	34.2 $\mu\text{g h}^{-1} \text{mg}^{-1}_{\text{cat}}$	This work
Au-TiO ₂ sub nanocluster	0.1 M HCl	25 °C	21.4 $\mu\text{g h}^{-1} \text{mg}^{-1}$	S1
Au nanorods	0.1 M KOH	25 °C	1.65 $\mu\text{g h}^{-1} \text{cm}^{-2}$	S2
Amorphous-Au-CeO _x -RGO	0.1 M HCl	25 °C	8.3 $\mu\text{g h}^{-1} \text{mg}^{-1}_{\text{cat}}$	S3
Li ⁺ -incorporation poly(Nethyl-benzene-1,2,4,5-tetracarboxylic diimide)	0.5 M Li ₂ SO ₄	25 °C	1.58 $\mu\text{g h}^{-1} \text{cm}^{-2}$	S4
amorphous Bi ₄ V ₂ O ₁₁ crystalline CeO ₂ hybrid nanofibers	0.1 M HCl	25 °C	23.21 $\mu\text{g h}^{-1} \text{mg}^{-1}$	S5
N-Doped Porous Carbon	0.05 M H ₂ SO ₄	25 °C	1.40 $\text{mmol g}^{-1} \text{h}^{-1}$	S6
Amorphous PdCu-rGO	0.1 M KOH	25 °C	2.8 $\mu\text{g h}^{-1} \text{mg}^{-1}_{\text{cat}}$	S7
Pd/C	0.1 M PBS	25 °C	4.9 $\mu\text{g mg}^{-1}_{\text{Pd}} \text{h}^{-1}$	S8
Rh nanosheets nanoassemblies	0.1 M KOH	25 °C	23.9 $\mu\text{g h}^{-1} \text{mg}^{-1}_{\text{cat}}$	S9
Hollow Gold Nanocages	0.5 M LiClO ₄	20 °C	2.35 $\mu\text{g cm}^{-2} \text{h}^{-1}$	S10

References

- [S1] M. M. Shi, D. Bao, B. R. Wulan, Y. H. Li, Y. F. Zhang, J. M. Yan and Q. Jiang, *Adv. Mater.*, 2017, **29**, 1606550.
- [S2] D. Bao, Q. Zhang, F. L. Meng, H. X. Zhong, M. M. Shi, Y. Zhang, J. M. Yan, Q. Jiang and X. B. Zhang, *Adv. Mater.*, 2017, **29**, 1604799.
- [S3] S. J. Li, D. Bao, M. M. Shi, B. R. Wulan, J. M. Yan and Q. Jiang, *Adv. Mater.*, 2017, **29**, 1700001.
- [S4] G. F. Chen, X. Cao, S. Wu, X. Zeng, L. X. Ding, M. Zhu and H. Wang, *J. Am. Chem. Soc.*, 2017, **139**, 9771-9774.
- [S5] C. Lv, C. Yan, G. Chen, Y. Ding, J. Sun, Y. Zhou and G. Yu, *Angew. Chem., Int. Ed.*, 2018, **57**, 6073-6076.
- [S6] Y. Liu, Y. Su, X. Quan, X. Fan, S. Chen, H. Yu, H. Zhao, Y. Zhang and J. Zhao, *ACS Catal.*, 2018, **8**, 1186-1191.
- [S7] M. M. Shi, D. Bao, S. J. Li, B. R. Wulan, J. M. Yan and Q. Jiang, *Adv. Energy Mater.*, 2018, **8**, 1800124.
- [S8] J. Wang, L. Yu, L. Hu, G. Chen, H. Xin and X. Feng, *Nat. Commun.*, 2018, **9**, 1795.
- [S9] H. M. Liu, S. H. Han, Y. Zhao, Y. Y. Zhu, X. L. Tian, J. H. Zeng, J. X. Jiang, B. Y. Xia and Y. Chen, *J. Mater. Chem. A*, 2018, **6**, 3211-3217.
- [S10] M. Nazemi, S. R. Panikkanvalappil and M. A. El-Sayed, *Nano Energy*, 2018, **49**, 316-323.